

Averaged Adam accelerates stochastic optimization in the training of deep neural network approximations for partial differential equation and optimal control problems

Steffen Dereich¹, Arnulf Jentzen^{2,3}, and Adrian Riekert⁴

¹ Institute for Mathematical Stochastics, University of Münster, Germany; e-mail: steffen.dereich@uni-muenster.de

² School of Data Science and Shenzhen Research Institute of Big Data, The Chinese University of Hong Kong, Shenzhen (CUHK-Shenzhen), China; e-mail: ajentzen@cuhk.edu.cn

³ Applied Mathematics: Institute for Analysis and Numerics, University of Münster, Germany; e-mail: ajentzen@uni-muenster.de

⁴ Applied Mathematics: Institute for Analysis and Numerics, University of Münster, Germany; e-mail: ariekert@uni-muenster.de

January 13, 2025

Abstract

Deep learning methods – usually consisting of a class of deep neural networks (DNNs) trained by a stochastic gradient descent (SGD) optimization method – are nowadays omnipresent in data-driven learning problems as well as in scientific computing tasks such as optimal control (OC) and partial differential equation (PDE) problems. In practically relevant learning tasks, often not the plain-vanilla standard SGD optimization method is employed to train the considered class of DNNs but instead more sophisticated adaptive and accelerated variants of the standard SGD method such as the popular Adam optimizer are used. Inspired by the classical Polyak–Ruppert averaging approach, in this work we apply averaged variants of the Adam optimizer to train DNNs to approximately solve exemplary scientific computing problems in the form of PDEs and OC problems. We test the averaged variants of Adam in a series of learning problems including physics-informed neural network (PINN), deep backward stochastic differential equation (deep BSDE), and deep Kolmogorov approximations for PDEs (such as heat, Black–Scholes, Burgers, and Allen–Cahn PDEs), including DNN approximations for OC problems, and including DNN approximations for image classification problems (ResNet for CIFAR-10). In each of the numerical

examples the employed averaged variants of Adam outperform the standard Adam and the standard SGD optimizers, particularly, in the situation of the scientific machine learning problems. The PYTHON source codes for the numerical experiments associated to this work can be found on GITHUB at <https://github.com/deeplearningmethods/averaged-adam>.

Contents

1	Introduction	2
2	Averaged Adam optimizers	4
2.1	Standard Adam optimizer	4
2.2	General averaged Adam optimizers	5
2.3	Partially arithmetically averaged Adam optimizer	7
2.4	Geometrically weighted averaged Adam optimizer	10
3	Numerical experiments	11
3.1	Introduction	11
3.2	Polynomial regression	11
3.3	Artificial neural network (ANN) approximations for explicitly given functions . .	12
3.3.1	ANN approximations for a 6-dimensional polynomial	12
3.3.2	ANN approximations for a 20-dimensional normal distribution	12
3.4	Deep Kolmogorov method (DKM)	13
3.4.1	Heat PDE	13
3.4.2	Black–Scholes PDE	14
3.5	Physics-informed neural networks (PINNs)	15
3.5.1	Allen-Cahn PDE	15
3.5.2	Sine-Gordon type PDE	16
3.5.3	Burgers equation	16
3.6	Deep BSDE method for a Hamiltonian–Jacobi–Bellman (HJB) equation	17
3.7	Optimal control problem	19
3.8	Image classification	19
4	Conclusion	20

1 Introduction

Deep learning (DL) methods are nowadays not only highly used to approximately solve data driven learning problems – such as those occurring in *artificial intelligence* (AI) based chatbot systems (cf., for instance, [8, 29]) and AI based text-to-image creation models (cf., for example,

[37, 39, 42]) – but DL methods are these days also extensively used to approximate solutions of scientific computing problems such as *partial differential equations* (PDEs) and *optimal control* (OC) problems (cf., for instance, the overview articles [7, 10, 18, 20, 24]).

DL methods typically consist of a class of deep *artificial neural networks* (ANNs) that are trained by a *stochastic gradient descent* (SGD) optimization method. In practically relevant learning problems, often not the plain-vanilla standard SGD optimization method is employed to train the considered class of deep ANNs but instead more sophisticated adaptive and accelerated variants of the standard SGD method are used (cf., for example, [4, 26, 40, 44] for overviews and monographs). Maybe the most popular variant of such adaptive and accelerated SGD methods is the famous *adaptive moment estimation SGD* (Adam) optimizer proposed in 2014 by Kingma & Ba (see [27]).

Inspired by the classical Polyak–Ruppert averaging approach [34, 41] (cf. also [35]), several averaged variants of SGD optimization methods have been considered in the literature as well. In particular, we refer, for instance, to [3, 9, 11, 21, 25, 31, 43, 45] and the references therein for works proposing and testing SGD methods involving suitable averaging techniques and we refer, for example, to [1, 2, 13, 15, 16, 19, 30] and the references therein for articles studying averaged variants of SGD methods analytically.

In this work we apply different averaged variants of the Adam optimizer (see Section 3) to train deep ANNs to approximately solve exemplary scientific computing and image classification problems. Specifically, we study the considered averaged variants of the Adam optimizer numerically in a series of learning problems

- including polynomial regression problems (see Subsection 3.2),
- including deep ANN approximations for explicitly given high-dimensional target functions (see Subsection 3.3),
- including *physics-informed neural network* (PINN) (see Subsection 3.5), *deep backward stochastic differential equation* (deep BSDE) (see Subsection 3.6), and *deep Kolmogorov* (DK) (see Subsection 3.4) approximations for PDEs (such as heat, Black–Scholes, Burgers, Allen–Cahn, and *Hamiltonian–Jacobi–Bellman* (HJB) PDEs),
- including deep ANN approximations for stochastic OC problems (see Subsection 3.7), and
- including residual deep ANN approximations for the CIFAR-10 image classification dataset (see Subsection 3.8).

In each of the considered numerical examples the suggested optimizers outperform the standard Adam and the standard SGD optimizers, particularly, in the situation of the considered scientific computing problems. Taking this into account, we strongly suggest to further study and employ averaged variants of the Adam optimizers when solving PDE, OC, or related scientific computing problems by means of deep learning approximation methods. The PYTHON source codes for each of the performed numerical simulations can be found on GITHUB at <https://github.com/deeplearningmethods/averaged-adam>.

Structure of this article

The remainder of this work is organized as follows. In Section 2 we recall the concept of the standard Adam optimizer and we describe in detail the specific averaged variants of the Adam optimizer that we employ in our numerical simulations. In Section 3 we apply the considered averaged variants of the Adam optimizer to several scientific computing and image classification problems and compare the obtained approximation errors with those of the standard SGD and the standard Adam optimizers. Finally, in Section 4 we briefly summarize the findings of this work and also outline directions of future research.

2 Averaged Adam optimizers

2.1 Standard Adam optimizer

For convenience of the reader we recall within this subsection in Definition 2.1 and Algorithm 1 below the concept of the “standard” Adam optimizer from Kingma & Ba [27]. Definition 2.1 is a modified variant of [26, Definition 7.9.1].

Definition 2.1 (Standard Adam optimizer). *Let $d, \mathcal{d} \in \mathbb{N}$, $(\gamma_n)_{n \in \mathbb{N}} \subseteq \mathbb{R}$, $(J_n)_{n \in \mathbb{N}} \subseteq \mathbb{N}$, $(\alpha_n)_{n \in \mathbb{N}} \subseteq [0, 1)$, $(\beta_n)_{n \in \mathbb{N}} \subseteq [0, 1)$, $\varepsilon \in (0, \infty)$, let $(\Omega, \mathcal{F}, \mathbb{P})$ be a probability space, for every $n, j \in \mathbb{N}$ let $X_{n,j}: \Omega \rightarrow \mathbb{R}^{\mathcal{d}}$ be a random variable, let $\ell: \mathbb{R}^d \times \mathbb{R}^{\mathcal{d}} \rightarrow \mathbb{R}$ be differentiable, let $\mathcal{g} = (\mathcal{g}_1, \dots, \mathcal{g}_{\mathcal{d}}): \mathbb{R}^d \times \mathbb{R}^{\mathcal{d}} \rightarrow \mathbb{R}^{\mathcal{d}}$ satisfy for all $\theta \in \mathbb{R}^d$, $x \in \mathbb{R}^{\mathcal{d}}$ that*

$$\mathcal{g}(\theta, x) = \nabla_{\theta} \ell(\theta, x), \quad (1)$$

and let $\Theta = (\Theta^{(1)}, \dots, \Theta^{(d)}): \mathbb{N}_0 \times \Omega \rightarrow \mathbb{R}^d$ be a function. Then we say that Θ is the Adam process for ℓ with hyperparameters $(\alpha_n)_{n \in \mathbb{N}}$, $(\beta_n)_{n \in \mathbb{N}}$, $(\gamma_n)_{n \in \mathbb{N}}$, $\varepsilon \in (0, \infty)$, batch-sizes $(J_n)_{n \in \mathbb{N}}$, initial value Θ_0 , and data $(X_{n,j})_{(n,j) \in \mathbb{N}^2}$ if and only if there exist $\mathbf{m} = (\mathbf{m}^{(1)}, \dots, \mathbf{m}^{(d)}): \mathbb{N}_0 \times \Omega \rightarrow \mathbb{R}^{\mathcal{d}}$ and $\mathbf{v} = (\mathbf{v}^{(1)}, \dots, \mathbf{v}^{(d)}): \mathbb{N}_0 \times \Omega \rightarrow \mathbb{R}^{\mathcal{d}}$ such that for all $n \in \mathbb{N}$, $i \in \{1, 2, \dots, d\}$ it holds that

$$\mathbf{m}_0 = 0, \quad \mathbf{m}_n = \alpha_n \mathbf{m}_{n-1} + (1 - \alpha_n) \left[\frac{1}{J_n} \sum_{j=1}^{J_n} \mathcal{g}(\Theta_{n-1}, X_{n,j}) \right], \quad (2)$$

$$\mathbf{v}_0 = 0, \quad \mathbf{v}_n^{(i)} = \beta_n \mathbf{v}_{n-1}^{(i)} + (1 - \beta_n) \left[\frac{1}{J_n} \sum_{j=1}^{J_n} \mathcal{g}_i(\Theta_{n-1}, X_{n,j}) \right]^2, \quad (3)$$

$$\text{and} \quad \Theta_n^{(i)} = \Theta_{n-1}^{(i)} - \gamma_n \left[\varepsilon + \left[\frac{\mathbf{v}_n^{(i)}}{(1 - \prod_{k=1}^n \beta_k)} \right]^{1/2} \right]^{-1} \left[\frac{\mathbf{m}_n^{(i)}}{(1 - \prod_{k=1}^n \alpha_k)} \right]. \quad (4)$$

In Definition 2.1 the hyperparameter γ can be referred to as *learning rate*, the hyperparameter α can be referred to as *momentum decay factor*, the hyperparameter β can be referred to

as *second moment decay factor*, and the hyperparameter ε can be referred to as *regularizing parameter* (cf., for instance, [26, Definition 7.9.1]). In PYTORCH the hyperparameters $(\alpha_n)_{n \in \mathbb{N}}$, $(\beta_n)_{n \in \mathbb{N}}$, $(\gamma_n)_{n \in \mathbb{N}}$, and ε for the Adam optimizer in Definition 2.1 are by default chosen to satisfy for all $n \in \mathbb{N}$ that $\alpha_n = 0.9$, $\beta_n = 0.999$, $\gamma_n = 0.001$, and $\varepsilon = 10^{-8}$ (cf., for example, [27, 36]). In Algorithm 1 below we present a pseudo-code for the standard Adam optimizer in Definition 2.1.

Algorithm 1: Standard Adam optimizer	
Setting:	The mathematical objects introduced in Definition 2.1
Input:	$N \in \mathbb{N}$
Output:	Adam process $\Theta_N \in \mathbb{R}^d$ after N steps
<pre> 1: $\theta \leftarrow \Theta_0$ 2: $\mathbf{m} \leftarrow 0$ 3: $\mathbf{v} \leftarrow 0$ 4: for $n \in \{1, 2, \dots, N\}$ do 5: $g \leftarrow (J_n)^{-1} \sum_{j=1}^{J_n} \mathcal{G}(\theta, X_{n,j})$ 6: $\mathbf{m} \leftarrow \alpha_n \mathbf{m} + (1 - \alpha_n)g$ 7: $\mathbf{v} \leftarrow \beta_n \mathbf{v} + (1 - \beta_n)g^{\otimes 2}$ # Square $g^{\otimes 2}$ is understood componentwise 8: $\hat{\mathbf{m}} \leftarrow \mathbf{m} / (1 - \prod_{k=1}^n \alpha_k)$ 9: $\hat{\mathbf{v}} \leftarrow \mathbf{v} / (1 - \prod_{k=1}^n \beta_k)$ 10: $\theta \leftarrow \theta - \gamma_n \hat{\mathbf{m}} \otimes (\hat{\mathbf{v}}^{\otimes(1/2)} + \varepsilon)^{\otimes(-1)}$ # Root $\hat{\mathbf{v}}^{\otimes(1/2)}$ is understood componentwise 11: end for 12: return θ </pre>	

We refer, for instance, to [5, 12, 14, 28, 38] and the references therein for error and convergence rate analyses for the Adam optimizer.

2.2 General averaged Adam optimizers

In order to be in the position to precisely describe the optimization methods that we employ in the numerical simulations in Section 3 below, we present in this subsection (see Definition 2.2 below) for the convenience of the reader a general class of averaged variants of the Adam optimizer.

Definition 2.2 (General averaged Adam optimizer). *Let $d, \mathcal{d} \in \mathbb{N}$, $(\gamma_n)_{n \in \mathbb{N}} \subseteq \mathbb{R}$, $(J_n)_{n \in \mathbb{N}} \subseteq \mathbb{N}$, $(\alpha_n)_{n \in \mathbb{N}} \subseteq [0, 1)$, $(\beta_n)_{n \in \mathbb{N}} \subseteq [0, 1)$, $(\delta_{n,m})_{(n,m) \in (\mathbb{N}_0)^2} \subseteq \mathbb{R}$, $\varepsilon \in (0, \infty)$, let $(\Omega, \mathcal{F}, \mathbb{P})$ be a probability space, for every $n, j \in \mathbb{N}$ let $X_{n,j}: \Omega \rightarrow \mathbb{R}^{\mathcal{d}}$ be a random variable, let $\ell: \mathbb{R}^d \times \mathbb{R}^{\mathcal{d}} \rightarrow \mathbb{R}$ be differentiable, and let $\Theta: \mathbb{N}_0 \times \Omega \rightarrow \mathbb{R}^d$ be a function. Then we say that Θ is the averaged Adam process with loss ℓ , learning rates $(\gamma_n)_{n \in \mathbb{N}}$, batch sizes $(J_n)_{n \in \mathbb{N}}$, momentum decay factors $(\alpha_n)_{n \in \mathbb{N}}$, second moment decay factors $(\beta_n)_{n \in \mathbb{N}}$, regularizing factor $\varepsilon \in (0, \infty)$, initial value Θ_0 , data $(X_{n,j})_{(n,j) \in \mathbb{N}^2}$, and averaging weights $(\delta_{n,m})_{(n,m) \in (\mathbb{N}_0)^2}$ if and only if there exists $\vartheta: \mathbb{N}_0 \times \Omega \rightarrow \mathbb{R}^d$ such that*

(i) it holds that ϑ is the *Adam* process with loss ℓ , learning rates $(\gamma_n)_{n \in \mathbb{N}}$, batch sizes $(J_n)_{n \in \mathbb{N}}$, momentum decay factors $(\alpha_n)_{n \in \mathbb{N}}$, second moment decay factors $(\beta_n)_{n \in \mathbb{N}}$, regularizing factor $\varepsilon \in (0, \infty)$, initial value Θ_0 , and data $(X_{n,j})_{(n,j) \in \mathbb{N}^2}$ (cf. Definition 2.1) and

(ii) it holds for all $n \in \mathbb{N}$ that

$$\Theta_n = \sum_{m=0}^n \delta_{n,m} \vartheta_m. \quad (5)$$

In the following list we present a few special cases of Definition 2.2 by choosing specific values for the family of averaging weights $\delta_{n,m} \in \mathbb{R}$, $(n, m) \in (\mathbb{N}_0)^2$, in (5).

(I) *Standard Adam*: Consider Definition 2.2 and assume for all $n, m \in \mathbb{N}_0$ that $\delta_{n,m} = \mathbb{1}_{\{n\}}(m)$. Then it holds for all $n \in \mathbb{N}_0$ that

$$\Theta_n = \vartheta_n \quad (6)$$

and, in this situation, the averaged *Adam* process in Definition 2.2 reduces to the standard *Adam* process in Definition 2.1.

(II) *Arithmetic average of Adam over the last A steps*: Consider Definition 2.2, let $A \in \mathbb{N}$, and assume for all $n, m \in \mathbb{N}_0$ that $\delta_{n,m} = (A+1)^{-1} \mathbb{1}_{[0,A]}(n-m)$. Then it holds for all $n \in \mathbb{N} \cap [A, \infty)$ that

$$\Theta_n = \frac{\sum_{k=n+1-A}^n \vartheta_k}{A}. \quad (7)$$

The choice in (7) is the subject of Definition 2.3, Algorithm 2, and Algorithm 3 in Subsection 2.3. Moreover, in the case where $A = 999$ in (7) we present in Section 3 a series of numerical simulations for this averaged variant of the *Adam* optimizer. We also refer to this type of averaging of the *Adam* optimizer as *partially arithmetically averaged Adam optimizer*.

(III) *Geometrically weighted averages of Adam*: Consider Definition 2.2, let $(\varrho_n)_{n \in \mathbb{N}} \subseteq \mathbb{R}$ satisfy for all $n \in \mathbb{N}$ that $\varrho_n = 1 - \delta_{n,n}$, and assume for all $n, m \in \mathbb{N}_0$ with $m < n$ that $\delta_{n,m} = (1 - \delta_{n,n})\delta_{n-1,m}$. Then it holds for all $n \in \mathbb{N}$ that

$$\begin{aligned} \Theta_n &= \sum_{k=0}^n \delta_{n,k} \vartheta_k = \left[\sum_{k=0}^{n-1} \delta_{n,k} \vartheta_k \right] + \delta_{n,n} \vartheta_n = \left[\sum_{k=0}^{n-1} (1 - \delta_{n,n}) \delta_{n-1,k} \vartheta_k \right] + \delta_{n,n} \vartheta_n \\ &= (1 - \delta_{n,n}) \Theta_{n-1} + \delta_{n,n} \vartheta_n = \varrho_n \Theta_{n-1} + (1 - \varrho_n) \vartheta_n. \end{aligned} \quad (8)$$

Therefore, we obtain for all $n \in \mathbb{N}$ that

$$\Theta_n = \left[\prod_{k=1}^n \varrho_k \right] \Theta_0 + \sum_{k=1}^n \left(\left[\prod_{v=k+1}^n \varrho_v \right] (1 - \varrho_k) \vartheta_k \right) \quad (9)$$

The choice in (8) is the subject of Definition 2.4 and Algorithm 4 in Subsection 2.4. Moreover, in the case where it holds for all $n \in \mathbb{N}$ that $\varrho_n = 1 - \delta_{n,n} = 0.999$ in (8) we present in Section 3 a series of numerical simulations for this averaged variant of the Adam optimizer. In the scientific literature the type of averaging in (8) is referred to as *exponential moving average* (EMA) (cf., for example, [1, 3, 9, 21, 25, 31, 43]).

- (IV) *Arithmetic average of Adam over all steps since the A-th step*: Consider Definition 2.2, let $A \in \mathbb{N}_0$, and assume for all $n, m \in \mathbb{N}_0$ that $\delta_{n,m} = (n + 1 - A)^{-1} \mathbb{1}_{[A,n]}(m)$. Then it holds for all $n \in \mathbb{N} \cap [A, \infty)$ that

$$\Theta_n = \frac{\sum_{k=A}^n \vartheta_k}{n + 1 - A} \quad (10)$$

Hence, we obtain for all $n \in \mathbb{N} \cap (A, \infty)$ that

$$\begin{aligned} \Theta_n &= \frac{\sum_{k=A}^n \Theta_k}{n + 1 - A} = \frac{\sum_{k=A}^{n-1} \Theta_k}{n + 1 - A} + \frac{\vartheta_n}{n + 1 - A} \\ &= \Theta_{n-1} \left[\frac{(n-1) + 1 - A}{n + 1 - A} \right] + \frac{\vartheta_n}{n + 1 - A} \\ &= \left[\frac{n - A}{n + 1 - A} \right] \Theta_{n-1} + \left(1 - \left[\frac{n - A}{n + 1 - A} \right] \right) \vartheta_n. \end{aligned} \quad (11)$$

- (V) *Arithmetic average of Adam over all previous steps*: Consider Definition 2.2 and assume for all $n, m \in \mathbb{N}_0$ that $\delta_{n,m} = (n + 1)^{-1}$. Then it holds for all $n \in \mathbb{N}$ that

$$\Theta_n = \frac{\sum_{k=0}^n \vartheta_k}{n + 1} \quad (12)$$

Combining this and (11) proves for all $n \in \mathbb{N}$ that

$$\Theta_n = \left[\frac{n}{n + 1} \right] \Theta_{n-1} + \left(1 - \left[\frac{n}{n + 1} \right] \right) \vartheta_n. \quad (13)$$

This type of averaging corresponds to the classical Polyak–Ruppert averaging approach (see [34, 35, 41]).

2.3 Partially arithmetically averaged Adam optimizer

As we employ the partially arithmetically averaged variant of the Adam optimizer in item (II) in Subsection 2.2 above in each of our numerical simulations in Section 3, we describe this type of averaging of Adam and its specific implementations in Definition 2.3, Algorithm 2, and Algorithm 3 within this subsection in more details.

Definition 2.3 (Partially arithmetically averaged Adam optimizer). Let $d, \mathcal{d}, A \in \mathbb{N}$, $(\gamma_n)_{n \in \mathbb{N}} \subseteq \mathbb{R}$, $(J_n)_{n \in \mathbb{N}} \subseteq \mathbb{N}$, $(\alpha_n)_{n \in \mathbb{N}} \subseteq [0, 1)$, $(\beta_n)_{n \in \mathbb{N}} \subseteq [0, 1)$, $\varepsilon \in (0, \infty)$, let $(\Omega, \mathcal{F}, \mathbb{P})$ be a probability space, for every $n, j \in \mathbb{N}$ let $X_{n,j}: \Omega \rightarrow \mathbb{R}^{\mathcal{d}}$ be a random variable, let $\ell: \mathbb{R}^{\mathcal{d}} \times \mathbb{R}^{\mathcal{d}} \rightarrow \mathbb{R}$ be differentiable, and let $\Theta: \mathbb{N}_0 \times \Omega \rightarrow \mathbb{R}^{\mathcal{d}}$ be a function. Then we say that Θ is the A -partially averaged Adam process with loss ℓ , learning rates $(\gamma_n)_{n \in \mathbb{N}}$, batch sizes $(J_n)_{n \in \mathbb{N}}$, momentum decay factors $(\alpha_n)_{n \in \mathbb{N}}$, second moment decay factors $(\beta_n)_{n \in \mathbb{N}}$, regularizing factor $\varepsilon \in (0, \infty)$, initial value Θ_0 , and data $(X_{n,j})_{(n,j) \in \mathbb{N}^2}$ if and only if there exists $\vartheta: \mathbb{N}_0 \times \Omega \rightarrow \mathbb{R}^{\mathcal{d}}$ such that

(i) it holds that ϑ is the Adam process with loss ℓ , learning rates $(\gamma_n)_{n \in \mathbb{N}}$, batch sizes $(J_n)_{n \in \mathbb{N}}$, momentum decay factors $(\alpha_n)_{n \in \mathbb{N}}$, second moment decay factors $(\beta_n)_{n \in \mathbb{N}}$, regularizing factor $\varepsilon \in (0, \infty)$, initial value Θ_0 , and data $(X_{n,j})_{(n,j) \in \mathbb{N}^2}$ and

(ii) it holds for all $n \in \mathbb{N} \cap [A, \infty)$ that

$$\Theta_n = \frac{1}{A} \left[\sum_{k=n+1-A}^n \vartheta_k \right]. \quad (14)$$

In the following we describe in Algorithms 2 and 3 two different concrete implementations of the method in Definition 2.3 above.

Algorithm 2: Adam with partial arithmetic averaging	
Setting:	The mathematical objects introduced in Definition 2.3
Input:	$N \in \mathbb{N}$
Output:	A -partially averaged Adam process $\Theta_N \in \mathbb{R}^{\mathcal{d}}$ after N steps
1:	$\vartheta \leftarrow \Theta_0$
2:	$\theta \leftarrow \Theta_0$
3:	$\phi_0 \leftarrow \Theta_0$
4:	$\mathbf{m} \leftarrow 0$
5:	$\mathbf{v} \leftarrow 0$
6:	for $n \in \{1, 2, \dots, N\}$ do
7:	$g \leftarrow (J_n)^{-1} \sum_{j=1}^{J_n} \mathcal{G}(\vartheta, X_{n,j})$
8:	$\mathbf{m} \leftarrow \alpha_n \mathbf{m} + (1 - \alpha_n) g$
9:	$\mathbf{v} \leftarrow \beta_n \mathbf{v} + (1 - \beta_n) g^{\otimes 2}$ <i># Square $g^{\otimes 2}$ is understood componentwise</i>
10:	$\hat{\mathbf{m}} \leftarrow \mathbf{m} / (1 - \prod_{k=1}^n \alpha_k)$
11:	$\hat{\mathbf{v}} \leftarrow \mathbf{v} / (1 - \prod_{k=1}^n \beta_k)$
12:	$\vartheta \leftarrow \vartheta - \gamma_n \hat{\mathbf{m}} \otimes (\hat{\mathbf{v}}^{\otimes (1/2)} + \varepsilon)^{\otimes (-1)}$ <i># Root $\hat{\mathbf{v}}^{\otimes (1/2)}$ is understood componentwise</i>
13:	$\theta \leftarrow \theta + A^{-1}(\vartheta - \phi_0)$ <i># Update averaged iterate</i>
14:	if $n < A$ then
15:	$\phi_i \leftarrow \vartheta$
16:	else


```

17:       $(\phi_0, \phi_1, \dots, \phi_{N-1}) \leftarrow (\phi_1, \phi_2, \dots, \phi_{N-1}, \vartheta)$            # Store previous  $N$  iterates
18:  end if
19: end for
20: return  $\theta$ 

```

Algorithm 2 has the disadvantage that one needs to store all previous A iterates. In the following pseudocode in Algorithm 3 below we decompose $A = K\mathbb{A}$ and only update the averages every \mathbb{A} steps. In this way one only needs to store the average over groups of \mathbb{A} iterates, i.e., K instead of $K\mathbb{A}$ additional parameter vectors. In our numerical simulations in Section 3 below we implement the method in Definition 2.3 using Algorithm 3, for instance, with the choice $K = 1$, $\mathbb{A} = 1000$, $A = 1000$ in Algorithm 3.

Algorithm 3: Adam with partial arithmetic averaging over groups

Setting: The mathematical objects introduced in Definition 2.3

Input: $K, \mathbb{A}, N \in \mathbb{N}$

Output: A -partially averaged Adam process $\Theta_N \in \mathbb{R}^d$ after N steps

```

1:  $\vartheta \leftarrow \Theta_0$ 
2:  $\theta \leftarrow \Theta_0$ 
3:  $\phi_0 \leftarrow \Theta_0$ 
4:  $\chi \leftarrow 0$ 
5:  $\mathbf{m} \leftarrow 0$ 
6:  $\mathbf{v} \leftarrow 0$ 
7: for  $n \in \{1, 2, \dots, N\}$  do
8:    $g \leftarrow (J_n)^{-1} \sum_{j=1}^{J_n} \mathcal{G}(\theta, X_{n,j})$ 
9:    $\mathbf{m} \leftarrow \alpha_n \mathbf{m} + (1 - \alpha_n)g$ 
10:   $\mathbf{v} \leftarrow \beta_n \mathbf{v} + (1 - \beta_n)g^{\otimes 2}$            # Square  $g^{\otimes 2}$  is understood componentwise
11:   $\hat{\mathbf{m}} \leftarrow \mathbf{m} / (1 - \prod_{k=1}^n \alpha_k)$ 
12:   $\hat{\mathbf{v}} \leftarrow \mathbf{v} / (1 - \prod_{k=1}^n \beta_k)$ 
13:   $\vartheta \leftarrow \vartheta - \gamma_n \hat{\mathbf{m}} \otimes (\hat{\mathbf{v}}^{\otimes (1/2)} + \varepsilon)^{\otimes (-1)}$    # Root  $\mathbf{v}^{\otimes (1/2)}$  is understood componentwise
14:   $\chi \leftarrow \chi + \mathbb{A}^{-1} \vartheta$            # Update average of group of  $\mathbb{A}$  iterates
15:  if  $n \equiv 0 \pmod{\mathbb{A}}$  then
16:     $\theta \leftarrow \theta + K^{-1}(\chi - \phi_0)$            # Update averaged iterate
17:    if  $n < K\mathbb{A}$  then
18:       $\phi_n \leftarrow \chi$ 
19:    else           # Store previous  $K$  group averages
20:       $(\phi_0, \phi_1, \dots, \phi_{K-1}) \leftarrow (\phi_1, \phi_2, \dots, \phi_{K-1}, \chi)$ 
21:    end if
22:     $\chi \leftarrow 0$ 
23:  end if

```

```

24: end for
25: return  $\theta$ 

```

2.4 Geometrically weighted averaged Adam optimizer

As we also use the geometrically weighted averaged variant of Adam in item (III) in Subsection 2.2 above in each of our numerical simulations in Section 3 below, we describe this type of averaging of Adam and its implementation in Definition 2.4 and Algorithm 4 within this subsection in more details.

Definition 2.4 (Geometrically weighted averaged Adam optimizer). *Let $d, \mathcal{d} \in \mathbb{N}$, $(\gamma_n)_{n \in \mathbb{N}} \subseteq \mathbb{R}$, $(J_n)_{n \in \mathbb{N}} \subseteq \mathbb{N}$, $(\alpha_n)_{n \in \mathbb{N}} \subseteq [0, 1)$, $(\beta_n)_{n \in \mathbb{N}} \subseteq [0, 1)$, $(\delta_n)_{n \in \mathbb{N}} \subseteq \mathbb{R}$, $\varepsilon \in (0, \infty)$, let $(\Omega, \mathcal{F}, \mathbb{P})$ be a probability space, for every $n, j \in \mathbb{N}$ let $X_{n,j}: \Omega \rightarrow \mathbb{R}^{\mathcal{d}}$ be a random variable, let $\ell: \mathbb{R}^d \times \mathbb{R}^{\mathcal{d}} \rightarrow \mathbb{R}$ be differentiable, let $\mathcal{g} = (\mathcal{g}_1, \dots, \mathcal{g}_{\mathcal{d}}): \mathbb{R}^d \times \mathbb{R}^{\mathcal{d}} \rightarrow \mathbb{R}^{\mathcal{d}}$ satisfy for all $\theta \in \mathbb{R}^d$, $x \in \mathbb{R}^{\mathcal{d}}$ that*

$$\mathcal{g}(\theta, x) = \nabla_{\theta} \ell(\theta, x), \quad (15)$$

and let $\Theta: \mathbb{N}_0 \times \Omega \rightarrow \mathbb{R}^d$ be a function. Then we say that Θ is the geometrically weighted averaged Adam process with loss ℓ , learning rates $(\gamma_n)_{n \in \mathbb{N}}$, batch sizes $(J_n)_{n \in \mathbb{N}}$, momentum decay factors $(\alpha_n)_{n \in \mathbb{N}}$, second moment decay factors $(\beta_n)_{n \in \mathbb{N}}$, regularizing factor $\varepsilon \in (0, \infty)$, initial value Θ_0 , data $(X_{n,j})_{(n,j) \in \mathbb{N}^2}$, and averaging weights $(\delta_n)_{n \in \mathbb{N}}$ if and only if there exists $\vartheta: \mathbb{N}_0 \times \Omega \rightarrow \mathbb{R}^d$ such that

(i) it holds that ϑ is the Adam process with loss ℓ , learning rates $(\gamma_n)_{n \in \mathbb{N}}$, batch sizes $(J_n)_{n \in \mathbb{N}}$, momentum decay factors $(\alpha_n)_{n \in \mathbb{N}}$, second moment decay factors $(\beta_n)_{n \in \mathbb{N}}$, regularizing factor $\varepsilon \in (0, \infty)$, initial value Θ_0 , and data $(X_{n,j})_{(n,j) \in \mathbb{N}^2}$ and

(ii) it holds for all $n \in \mathbb{N}$ that

$$\Theta_n = \delta_n \Theta_{n-1} + (1 - \delta_n) \vartheta_n. \quad (16)$$

Algorithm 4: Adam with geometrically weighted averaging

Setting: The mathematical objects introduced in Definition 2.4

Input: $N \in \mathbb{N}$

Output: Geometrically weighted averaged Adam process $\Theta_N \in \mathbb{R}^d$ after N steps

```

1:  $\vartheta \leftarrow \Theta_0$ 
2:  $\theta \leftarrow \Theta_0$ 
3:  $\mathbf{m} \leftarrow 0$ 
4:  $\mathbf{v} \leftarrow 0$ 
5: for  $n \in \{1, 2, \dots, N\}$  do
6:    $g \leftarrow (J_n)^{-1} \sum_{j=1}^{J_n} \mathcal{g}(\vartheta, X_{n,j})$ 
7:    $\mathbf{m} \leftarrow \alpha_n \mathbf{m} + (1 - \alpha_n) g$ 

```

8:	$\mathbf{v} \leftarrow \beta_n \mathbf{m} + (1 - \beta_n) g^{\otimes 2}$	<i># Square $g^{\otimes 2}$ is understood componentwise</i>
9:	$\hat{\mathbf{m}} \leftarrow \mathbf{m} / (1 - \prod_{k=1}^n \alpha_k)$	
10:	$\hat{\mathbf{v}} \leftarrow \mathbf{v} / (1 - \prod_{k=1}^n \beta_k)$	
11:	$\vartheta \leftarrow \vartheta - \gamma_n \hat{\mathbf{m}} / (\hat{\mathbf{v}}^{\otimes (1/2)} + \varepsilon)$	<i># Root $\mathbf{v}^{\otimes (1/2)}$ is understood componentwise</i>
12:	$\theta \leftarrow \delta_n \theta + (1 - \delta_n) \vartheta$	<i># Update averaged iterate</i>
13:	end for	
14:	return θ	

In the scientific literature the averaging procedure described in Definition 2.4 and Algorithm 4 above is typically referred to as **EMA**. In particular, we refer, for example, to [31, 43] for numerical experiments for **EMA**, we refer, for instance, to [1] for convergence analyses of **EMA** in conjunction with **Adam**, and we refer, for example, to [9] for *stochastic differential equation* (**SDE**) limits of **SGD** methods with **EMA**.

3 Numerical experiments

3.1 Introduction

We tested the two averaged variants of the **Adam** optimizer in Algorithm 3 (see Definition 2.3) and Algorithm 4 (see Definition 2.4). Specifically, we employed Algorithm 3 with $A \in \{100, 1000\}$ and Algorithm 4 with $\forall n \in \mathbb{N}: \delta_n = \delta_1 \in \{0.99, 0.999\}$, where $\delta_1 = 0.999$ seemed to work best in most cases.

All of the experiments were implemented in the machine learning library **PYTORCH** (cf., for instance, [32, 33]). The **PYTHON** source codes for each of the performed numerical simulations can be found on **GITHUB** at <https://github.com/deeplearningmethods/averaged-adam>.

3.2 Polynomial regression

As a first example we consider a simple regression problem with data corrupted by random noise. We optimize the coefficients of a polynomial with degree at most 25 to approximate the function $[-1, 1] \ni x \mapsto \sin(\pi x) \in \mathbb{R}$ in $L^2([-1, 1]; \mathbb{R})$. In other words, we attempt to minimize the function

$$\mathbb{R}^{d+1} \ni \theta = (\theta_0, \theta_1, \dots, \theta_d) \mapsto \int_{-1}^1 |\sin(\pi x) - \sum_{k=0}^d \theta_k x^k|^2 dx \in \mathbb{R} \quad (17)$$

for $d = 25$, leading to an 26-dimensional convex optimization problem. For the training we use a batch size of 64 and constant learning rates of size 10^{-2} and we add random noise to the output following a centered Gaussian distribution with variance $1/5$. Here and in most of the following numerical experiments we compare the plain vanilla **SGD** method, the standard **Adam** optimizer, **Adam** with partial arithmetic averaging (Algorithm 3) with $A = 1000$, and **Adam**

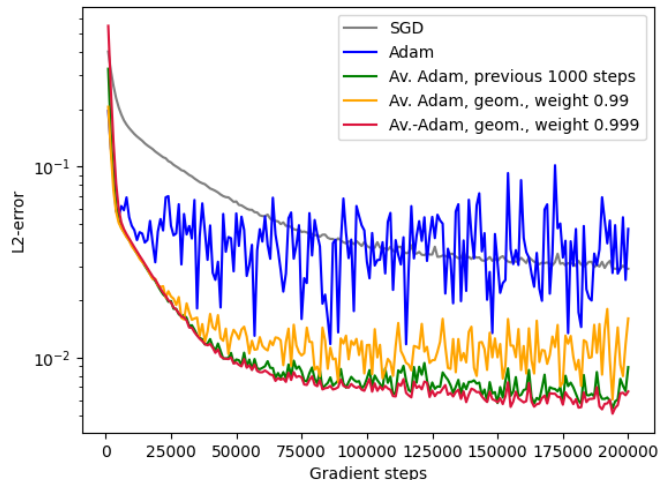


Figure 1: Numerical results for the polynomial regression problem described in Subsection 3.2.

with geometrically weighted averaging (Algorithm 4) with $\forall n \in \mathbb{N}: \delta_n = \delta_1 \in \{0.99, 0.999\}$. The results are visualized in Figure 1.

3.3 Artificial neural network (ANN) approximations for explicitly given functions

3.3.1 ANN approximations for a 6-dimensional polynomial

We train standard fully connected feedforward ANNs to approximate the target function

$$[-1, 1]^d \ni x = (x_1, \dots, x_d) \mapsto 1 + \sum_{i=1}^d (d + 1 - 2i)(x_i)^3 \in \mathbb{R} \quad (18)$$

for $d = 6$. We use ANNs with the *rectified linear unit* (ReLU) activation and two hidden layers consisting of 64 neurons each. As the input distribution we choose the continuous uniform distribution on $[-1, 1]^d$. We use a batch size of 256 and constant learning rates of size 10^{-2} . The results are visualized in Figure 2.

3.3.2 ANN approximations for a 20-dimensional normal distribution

As a further example we train fully connected feedforward ANNs to approximate the unnormalized density function

$$[-2, 2]^d \ni x \mapsto \exp\left(-\frac{\|x\|^2}{6}\right) \in \mathbb{R} \quad (19)$$

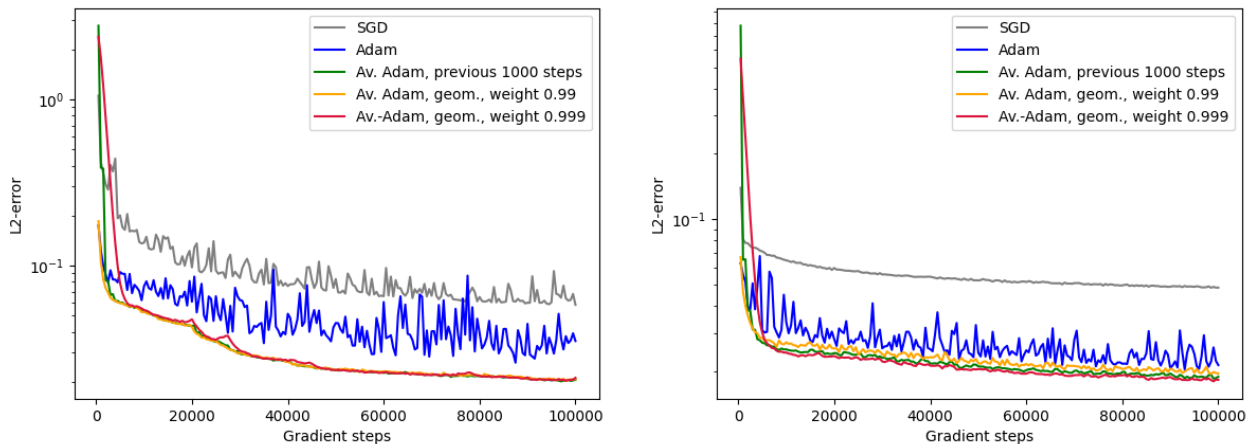


Figure 2: Results for the supervised learning problem for the target functions in (18) (left) and (19) (right).

in $d = 20$ dimensions. We use ANNs with the ReLU activation and three hidden layers consisting of 50, 100, and 50 neurons, respectively. As the input distribution we choose the continuous uniform distribution on $[-2, 2]^d$. For the training we employ the Adam optimizer with a batch size of 256 and constant learning rates of size 10^{-3} . Again we add random noise to the output following a centered Gaussian distribution with variance $1/5$. The results are visualized in Figure 2.

3.4 Deep Kolmogorov method (DKM)

Within this subsection we use the *deep Kolmogorov method* (DKM) proposed in Beck et al. [6] to solve different linear PDEs.

3.4.1 Heat PDE

We first consider the heat PDE on \mathbb{R}^d for $d = 10$. Specifically, we consider $d = 10$ and we attempt to approximate the solution $u: [0, T] \times \mathbb{R}^d \rightarrow \mathbb{R}$ of the PDE

$$\frac{\partial u}{\partial t} = \Delta_x u, \quad u(0, x) = \|x\|^2 \quad (20)$$

for $t \in [0, T]$, $x \in \mathbb{R}^d$ at the final time $T = 2$ on the domain $[-1, 1]^d$. The PDE can be reformulated as a stochastic minimization problem (cf. Beck et al. [6]) and thus SGD methods such as the Adam optimizer can be used to compute an approximate minimizer. We employ fully connected feedforward ANNs with three hidden layers consisting of 50, 100, and 50 neurons, respectively. This time we use the smooth *Gaussian error linear unit* (GELU) activation,

which seems to be more suitable for PDE problems. We tested both constant learning rates of size $5 \cdot 10^{-4}$ and polynomially decaying learning rates of size $\gamma_n = 5 \cdot 10^{-3} \cdot n^{-1/4}$, and a batch size of 2048. To compute the test error we compare the output with the exact solution $u(t, x) = \|x\|^2 + 2dt$ for $t \in [0, T]$, $x \in \mathbb{R}^d$. The results are visualized in Figure 3.

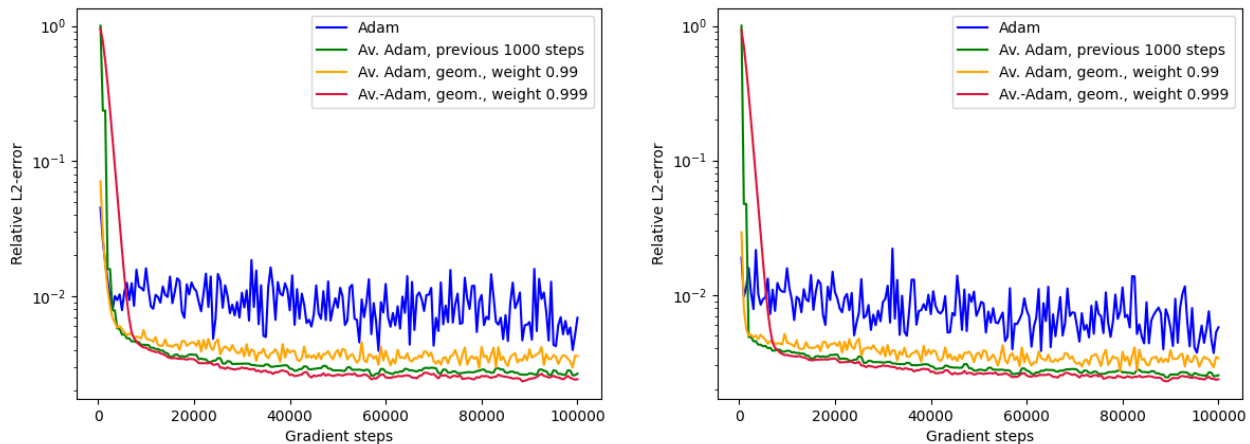


Figure 3: Results for the heat PDE in (20) using the DKM with constant learning rates (left) and decreasing learning rates (right).

3.4.2 Black–Scholes PDE

We next consider a Black–Scholes PDE on $[90, 110]^d$ for $d = 20$. Specifically, we consider $d = 20$ and we attempt to approximate the solution $u: [0, T] \times \mathbb{R}^d \rightarrow \mathbb{R}$ of the PDE

$$\frac{\partial u}{\partial t} = \frac{1}{2} \sum_{i=1}^d |\sigma_i x_i|^2 \frac{\partial^2 u}{\partial x_i^2} + \mu \sum_{i=1}^d x_i \frac{\partial u}{\partial x_i}, \quad u(0, x) = \exp(-rT) \max\{\max\{x_1, x_2, \dots, x_d\} - K, 0\} \quad (21)$$

for $t \in [0, T]$, $x = (x_1, \dots, x_d) \in \mathbb{R}^d$ where $\sigma = (\sigma_i)_{i \in \{1, 2, \dots, d\}} = (\frac{i+1}{2d})_{i \in \{1, 2, \dots, d\}}$, $r = -\mu = \frac{1}{20}$, $K = 100$ at the final time $T = 1$ using the DKM. We again employ fully connected feedforward ANNs with the GELU activation and three hidden layers consisting of 50, 100, and 50 neurons, respectively, and a batch normalization layer before the first hidden layer. For the training we use the batch size 2048 and test two different learning rate schedules: Constant learning rates of size $5 \cdot 10^{-4}$ and slowly decreasing learning rates of the form $\gamma_n = 5 \cdot 10^{-3} \cdot n^{-1/4}$ (see Figure 4), which lead to comparable results. To compute the test error we compare the output with the exact solution computed with the Feynman–Kac formula and approximated using a Monte Carlo method with 2048000 Monte Carlo samples.

As a second example we consider a Black–Scholes PDE with correlated noise on $[90, 110]^d$ for $d = 20$. Specifically, let $d = 20$ and let $Q = (Q_{i,j})_{(i,j) \in \{1, 2, \dots, d\}^2}$, $\Sigma = (\Sigma_{i,j})_{(i,j) \in \{1, 2, \dots, d\}^2} \in \mathbb{R}^{d \times d}$,

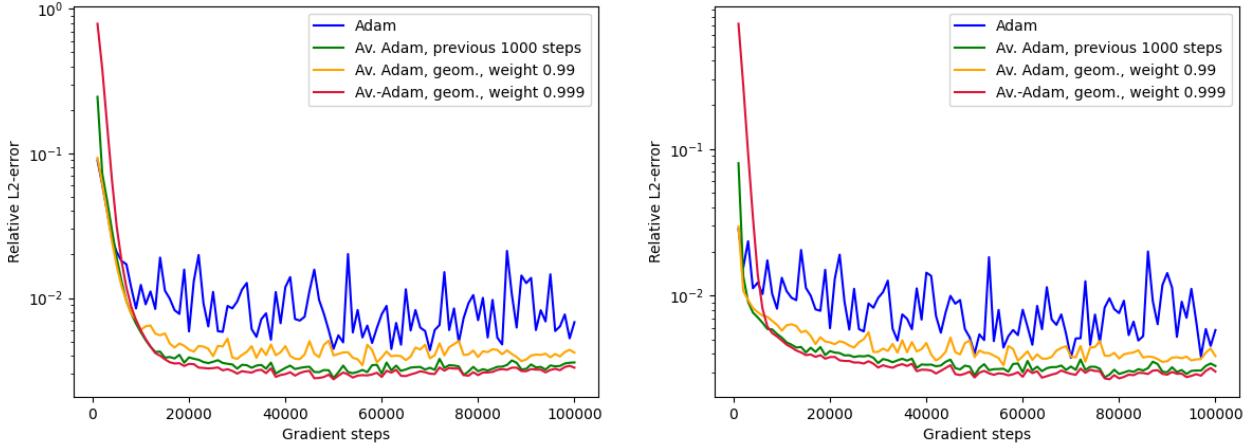


Figure 4: Results for the Black-Scholes PDE in (21) using the DKM, with constant learning rates (left) and decreasing learning rates (right).

$\beta = (\beta_1, \dots, \beta_d)$, $\zeta_1, \zeta_2, \dots, \zeta_d \in \mathbb{R}^d$ satisfy for all $i, j, k \in \{1, 2, \dots, d\}$ with $i < j$ that $\beta_k = \frac{1}{10} + \frac{k}{2d}$, $Q_{k,k} = 1$, $Q_{i,j} = Q_{j,i} = \frac{1}{2}$, $\Sigma_{i,j} = 0$, $\Sigma_{k,k} > 0$, $\Sigma\Sigma^* = Q$, and $\zeta_k = (\beta_k \Sigma_{k,1}, \beta_k \Sigma_{k,2}, \dots, \beta_k \Sigma_{k,d})$ (cf. [6, Section 4.4]). We attempt to approximate the solution $u: [0, T] \times \mathbb{R}^d \rightarrow \mathbb{R}$ of the PDE

$$\frac{\partial u}{\partial t} = \frac{1}{2} \sum_{i,j=1}^d x_i x_j \langle \zeta_i, \zeta_j \rangle \frac{\partial^2 u}{\partial x_i \partial x_j} + \mu \sum_{i=1}^d x_i \frac{\partial u}{\partial x_i}, \quad (22)$$

$$u(0, x) = \exp(-rT) \max\{K - \min\{x_1, x_2, \dots, x_d\}, 0\}$$

for $t \in [0, T]$, $x = (x_1, \dots, x_d) \in \mathbb{R}^d$ where $r = -\mu = \frac{1}{20}$, $K = 110$ at the final time $T = 1$ using the DKM. The remaining hyperparameters for the experiment are the same as for the Black-Scholes PDE in (21). The results are visualized in Figure 5.

3.5 Physics-informed neural networks (PINNs)

We used the method of PINNs to approximately solve a few semilinear heat PDEs.

3.5.1 Allen-Cahn PDE

We first consider the Allen-Cahn PDE on the domain $D = [0, 2] \times [0, 1]$ with time horizon $T = 4$. Specifically, we attempt to approximate the solution $u: [0, T] \times D \rightarrow \mathbb{R}$ of the PDE

$$\frac{\partial u}{\partial t} = \frac{1}{100} \Delta_x u + (u - u^3), \quad u(0, x) = \sin(\pi x_1) \sin(\pi x_2) \quad (23)$$

for $t \in [0, T]$, $x = (x_1, x_2) \in D$ equipped with Dirichlet boundary conditions at the terminal time $T = 4$. We used fully connected feedforward ANNs with 3 hidden layers consisting of

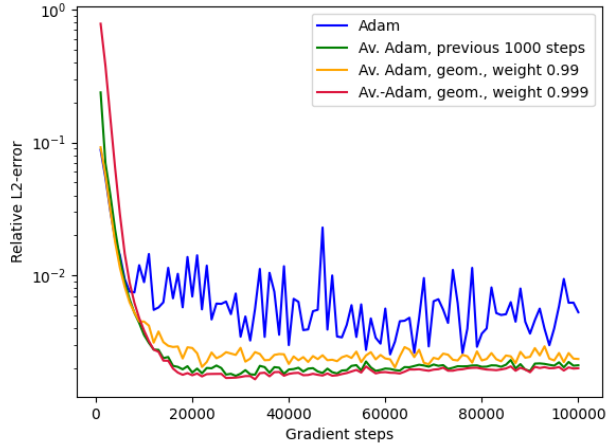


Figure 5: Results for the Black-Scholes PDE in (22) using the DKM.

32, 64, and 32 neurons, respectively, and the GELU activation. For the training we employ the Adam optimizer with a batch size of 256 and constant learning rates of size 10^{-3} . To compute the test error we compare the output with a reference solution obtained by a finite element method using 101^2 degrees of freedom in space and 500 second order linear implicit Runge-Kutta time steps. The results are visualized in Figure 6.

3.5.2 Sine-Gordon type PDE

We next consider a Sine-Gordon type semilinear PDE on the domain $D = [0, 2] \times [0, 1]$ with time horizon $T = 1$. Specifically, we attempt to approximate the solution $u: [0, T] \times D \rightarrow \mathbb{R}$ of the PDE

$$\frac{\partial u}{\partial t} = \frac{1}{20} \Delta_x u + \sin(u), \quad u(0, x) = \frac{3}{2} |\sin(\pi x_1) \sin(\pi x_2)|^2 \quad (24)$$

for $t \in [0, T]$, $x = (x_1, x_2) \in D$ equipped with Dirichlet boundary conditions at the terminal time $T = 1$. The other hyperparameters for the training are the same as in the case of the Allen-Cahn PDE. The results are visualized in Figure 6.

3.5.3 Burgers equation

We also employ the PINN method to approximately solve the one-dimensional Burgers equation

$$\frac{\partial u}{\partial t} = \alpha \Delta_x u - u \frac{\partial u}{\partial x}, \quad u(0, x) = \frac{2\alpha\pi \sin(\pi x)}{\beta + \cos(\pi x)} \quad (25)$$

for $t \in [0, T]$, $x \in D = [0, 2]$ equipped with Dirichlet boundary conditions at the terminal time $T = \frac{1}{2}$, where $\alpha = \frac{1}{20}$ and $\beta = \frac{11}{10}$. The exact solution satisfies for all $t \in [0, T]$, $x \in D$ that $u(t, x) = \frac{2\alpha\pi \sin(\pi x)}{\beta \exp(\alpha t \pi^2) + \cos(\pi x)}$.

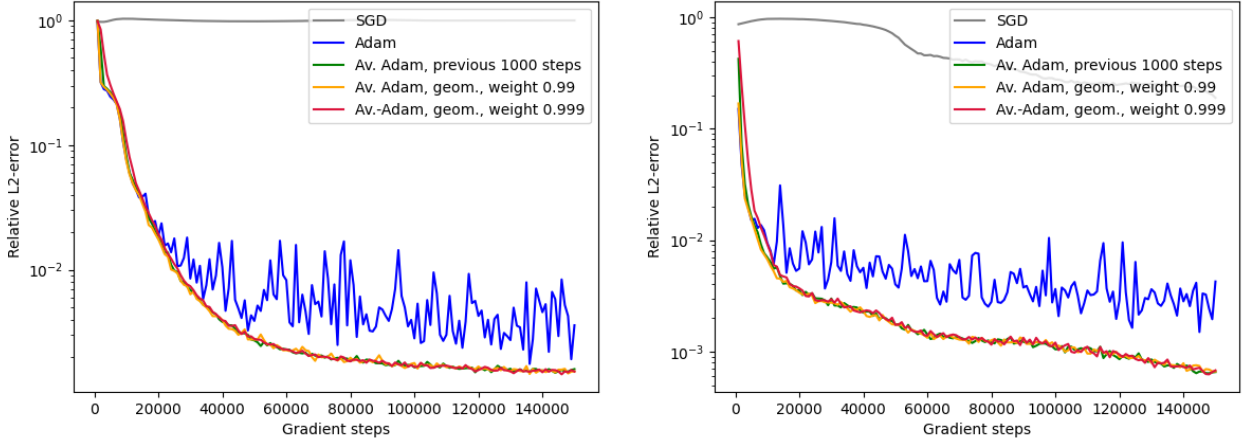


Figure 6: Results for the Allen-Cahn PDE in (23) (left) and the Sine-Gordon PDE in (24) (right) using PINNs.

We use fully connected feedforward ANNs with 3 hidden layers consisting of 16, 32, and 16 neurons, respectively, and the GELU activation. For the training we employ the Adam optimizer with a batch size of 128 and constant learning rates of size $3 \cdot 10^{-3}$. The results are visualized in Figure 7.

3.6 Deep BSDE method for a Hamiltonian–Jacobi–Bellman (HJB) equation

We employ the deep BSDE method introduced in E et al. [17, 22] to approximate the solution $u: [0, T] \times \mathbb{R}^d \rightarrow \mathbb{R}$ of the Hamilton–Jacobi–Bellman PDE

$$\frac{\partial u}{\partial t} = -\Delta_x u + \|\nabla_x u\|^2, \quad u(T, x) = \ln\left(\frac{1}{2}(\|x\|^2 + 1)\right) \quad (26)$$

for $t \in [0, T]$, $x \in \mathbb{R}^d$ at initial time 0 for the time horizon $T = 1/4$ and dimension $d = 25$. We approximately solve the PDE on the domain $[-1, 1]^d$ using an ANN with two hidden layers consisting of 45 neurons each and the GELU activation. We employ a time discretization with $N = 20$ time steps and approximate the gradient of the solution at each time step using an ANN with two hidden layers consisting of 45 neurons each and the GELU activation.

For the training we employ the Adam optimizer with a batch size of 512 and slowly decreasing learning rates of the form $\gamma_n = 0.02 \cdot n^{-1/5}$. To compute the test error we compare the output with an approximation of the exact solution computed through a Monte Carlo approximation with 819200 Monte Carlo samples for the Cole–Hopf transform (cf., for example, [17, Lemma 4.2]). The results are visualized in Figure 8.

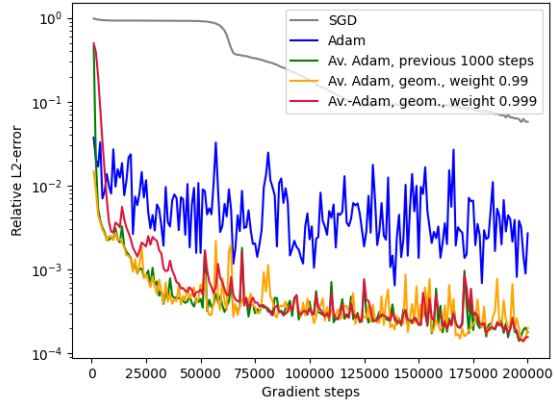


Figure 7: Results for the Burgers PDE in (25) using PINNs.

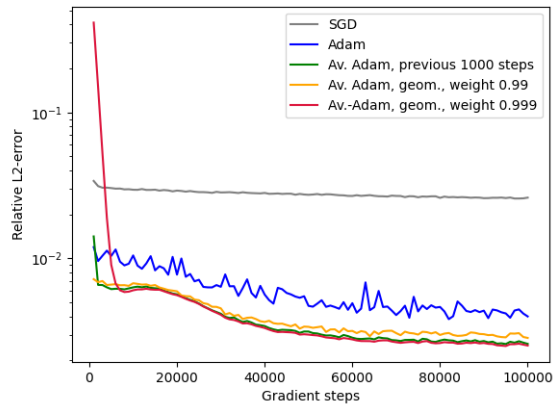


Figure 8: Results for the PDE in (26) using the deep BSDE method.

3.7 Optimal control problem

We consider a controlled diffusion of the form

$$dX_t = (AX_t + Bu_t) dt + \sqrt{2} dW_t \quad (27)$$

for $t \in [0, \infty)$ where $d \in \mathbb{N}$, where $X: [0, \infty) \times \Omega \rightarrow \mathbb{R}^d$ is the diffusion process, where $u: [0, \infty) \times \Omega \rightarrow \mathbb{R}^d$ is the control process, and where $A, B \in \mathbb{R}^{d \times d}$ are given matrices. We define the cost functional

$$J(t, x, u) = \mathbb{E} \left[\int_t^T (\frac{1}{2} \|X_s\|^2 + \|u_s\|^2) ds + \|X_T\|^2 \middle| X_t = x \right] \quad (28)$$

and attempt to compute the minimal expected cost

$$\inf_u \mathbb{E}[J(0, Z, u)], \quad (29)$$

where $Z: \Omega \rightarrow [-1, 1]^d$ is assumed to be continuous uniformly distributed. To this end, let $M \in \mathbb{N}$, $t_0, t_1, \dots, t_M \in \mathbb{R}$ satisfy for all $k \in \{1, 2, \dots, M\}$ that $t_k = \frac{kT}{N}$. We approximate the solution of the SDE in (27) with a forward Euler method. For each $n \in \{0, 1, \dots, N-1\}$ we approximate the control u_{t_n} through $u_{t_n} \approx \mathcal{N}^{\theta_n}(X_{t_n})$ where $\mathcal{N}^{\theta_n}: \mathbb{R}^d \rightarrow \mathbb{R}^d$ is the realization function of a neural network with parameter vector θ_n . In our experiment we use the values $d = 10$, $T = 1$, $N = 100$, and ANNs with 2 hidden layers consisting of 40 neurons each and the GELU activation. Additionally, we employ batch normalization after the input layer and each hidden layer. We train these neural networks using the Adam optimizer with a batch size of 1024 and constant learning rates of size 10^{-2} .

To compute the test error we approximate the expectation in (29) with 4096 Monte Carlo samples for Z and 500 Monte Carlo samples for the Brownian motion W and compare the output with the exact solution obtained by solving the corresponding Riccati *ordinary differential equation* (ODE) with 100000 time steps.

This time we compare the plain vanilla SGD method, the standard Adam optimizer, Adam with partial arithmetic averaging (Algorithm 3) with $A = 100$, and Adam with geometrically weighted averaging (Algorithm 4) with $\forall n \in \mathbb{N}: \delta_n = \delta_1 \in \{0.99, 0.999\}$. The results are visualized in Figure 9.

3.8 Image classification

We train a *residual neural network* (ResNet) on the CIFAR-10 dataset, a standard benchmark problem for image classification. Specifically, we use a variant of the ResNet architecture described in He et al. [23] with 9 layers, following the implementation at <https://github.com/matthias-wright/cifar10-resnet>. We employ the Adam optimizer with a batch size of 64, constant learning rates of size $2 \cdot 10^{-4}$, and weight decay with decay parameter $3 \cdot 10^{-4}$. Following standard ideas from data augmentation, we apply random horizontal flips with probability $1/2$, random offset cropping down to 32×32 , using reflection padding of 4 pixels, random color

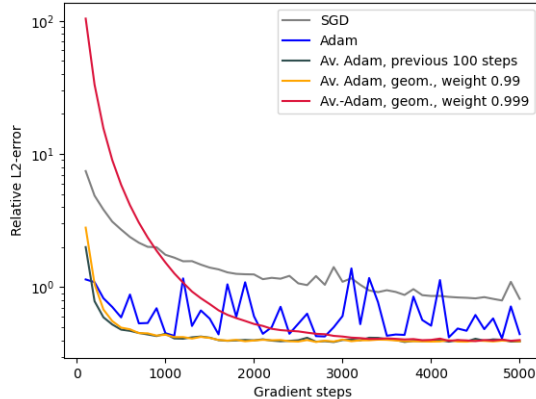


Figure 9: Results for the optimal control problem in (29).

jitter, and random rotations by an angle sampled uniformly from the interval $(0, \pi/4)$, to the training data. For details we refer to the documentation of PYTORCH transforms. The results are visualized in Figure 10.

4 Conclusion

In this work we have applied different averaged variants of the Adam optimizer (see Section 2) to a series of learning problems including polynomial regression problems (see Subsection 3.2), including deep ANN approximations for explicitly given high-dimensional target functions (see Subsection 3.3), including deep ANN approximations for stochastic OC problems (see Subsection 3.7), including DK (see Subsection 3.4), PINN (see Subsection 3.5), and deep BSDE (see Subsection 3.6) approximations for PDEs, and including residual deep ANN approximations for the CIFAR-10 image classification dataset (see Subsection 3.8). In each of the considered numerical examples the employed averaged variants of the Adam optimizer outperform the standard Adam and the standard SGD optimizers, particularly, in the situation of the considered scientific computing problems. Taking this into account, we believe that it is very relevant to further study and employ averaged variants of the Adam and similar optimizers, particularly, when solving PDE, OC, or related scientific computing problems by means of deep learning approximation methods.

Acknowledgments

This work has been partially funded by the European Union (ERC, MONTECARLO, 101045811). The views and the opinions expressed in this work are however those of the authors only and do

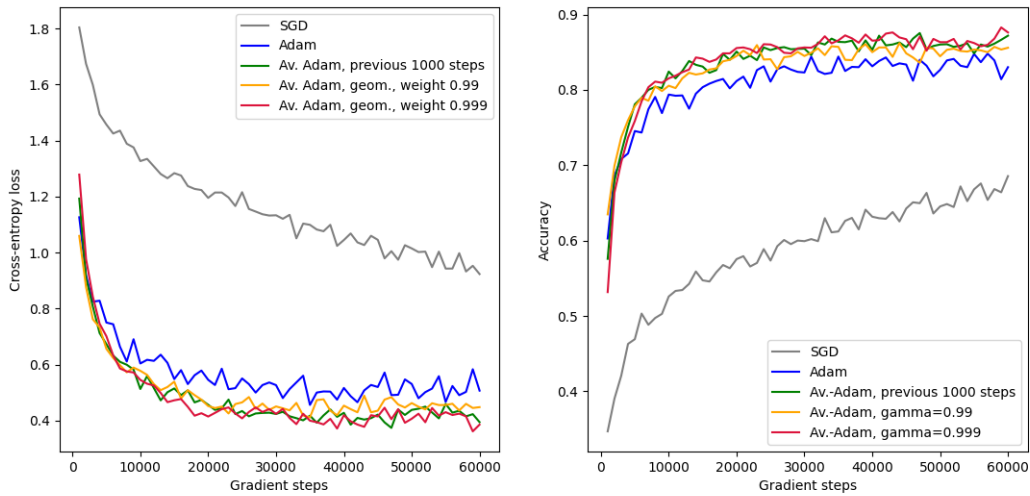


Figure 10: Results for the CIFAR-10 image classification problem using a ResNet. Left: test error, right: test accuracy.

not necessarily reflect those of the European Union or the European Research Council (ERC). Neither the European Union nor the granting authority can be held responsible for them. In addition, this work has been partially funded by the Deutsche Forschungsgemeinschaft (DFG, German Research Foundation) under Germany’s Excellence Strategy EXC 2044-390685587, Mathematics Münster: Dynamics-Geometry-Structure. Moreover, this work has been partially supported by the Ministry of Culture and Science NRW as part of the Lamarr Fellow Network.

References

- [1] AHN, K., AND CUTKOSKY, A. Adam with model exponential moving average is effective for nonconvex optimization. [arXiv:2405.18199](#) (2024), 25 pages.
- [2] AHN, K., MAGAKYAN, G., AND CUTKOSKY, A. General framework for online-to-nonconvex conversion: Schedule-free SGD is also effective for nonconvex optimization. [arXiv:2411.07061](#) (2024), 32 pages.
- [3] ATHIWARATKUN, B., FINZI, M., IZMAILOV, P., AND WILSON, A. G. There are many consistent explanations of unlabeled data: Why you should average. In *International Conference on Learning Representations* (2019).

- [4] BACH, F. *Learning Theory from First Principles*. Adaptive Computation and Machine Learning series. MIT Press, 2024.
- [5] BARAKAT, A., AND BIANCHI, P. Convergence and dynamical behavior of the Adam algorithm for nonconvex stochastic optimization. *SIAM J. Optim.* 31, 1 (2021), 244–274.
- [6] BECK, C., BECKER, S., GROHS, P., JAAFARI, N., AND JENTZEN, A. Solving the Kolmogorov PDE by means of deep learning. *Journal of Scientific Computing* 88, 3 (2021).
- [7] BECK, C., HUTZENTHALER, M., JENTZEN, A., AND KUCKUCK, B. An overview on deep learning-based approximation methods for partial differential equations. *Discrete Contin. Dyn. Syst. Ser. B* 28, 6 (2023), 3697–3746.
- [8] BROWN, T., MANN, B., RYDER, N., SUBBIAH, M., KAPLAN, J. D., DHARIWAL, P., NEELAKANTAN, A., SHYAM, P., SASTRY, G., ASKELL, A., AGARWAL, S., HERBERT-VOSS, A., KRUEGER, G., HENIGHAN, T., CHILD, R., RAMESH, A., ZIEGLER, D., WU, J., WINTER, C., HESSE, C., CHEN, M., SIGLER, E., LITWIN, M., GRAY, S., CHES, B., CLARK, J., BERNER, C., MCCANDLISH, S., RADFORD, A., SUTSKEVER, I., AND AMODEI, D. Language Models are Few-Shot Learners. In *Advances in Neural Information Processing Systems* (2020), H. Larochelle, M. Ranzato, R. Hadsell, M. Balcan, and H. Lin, Eds., vol. 33, Curran Associates, Inc., pp. 1877–1901.
- [9] BUSBRIDGE, D., RAMAPURAM, J., ABLIN, P., LIKHOMANENKO, T., DHEKANE, E. G., SUAU CUADROS, X., AND WEBB, R. How to scale your EMA. In *Advances in Neural Information Processing Systems* (2023), A. Oh, T. Naumann, A. Globerson, K. Saenko, M. Hardt, and S. Levine, Eds., vol. 36, Curran Associates, Inc., pp. 73122–73174.
- [10] CUOMO, S., SCHIANO DI COLA, V., GIAMPAOLO, F., ROZZA, G., RAISSI, M., AND PICCIALLI, F. Scientific machine learning through physics-informed neural networks: where we are and what’s next. *J. Sci. Comput.* 92, 3 (2022), Paper No. 88, 62.
- [11] DEFAZIO, A., YANG, X. A., MEHTA, H., MISHCHENKO, K., KHALED, A., AND CUTKOSKY, A. The Road Less Scheduled. [arXiv:2405.15682](https://arxiv.org/abs/2405.15682) (2024), 29 pages.
- [12] DÉFOSSEZ, A., BOTTOU, L., BACH, F., AND USUNIER, N. A Simple Convergence Proof of Adam and Adagrad. *Transactions on Machine Learning Research* (2022).
- [13] DEREICH, S. General multilevel adaptations for stochastic approximation algorithms II: CLTs. *Stochastic Process. Appl.* 132 (2021), 226–260.
- [14] DEREICH, S., AND JENTZEN, A. Convergence rates for the Adam optimizer. [arXiv:2407.21078](https://arxiv.org/abs/2407.21078) (2024), 43 pages.
- [15] DEREICH, S., AND KASSING, S. Central limit theorems for stochastic gradient descent with averaging for stable manifolds. *Electron. J. Probab.* 28 (2023), Paper No. 57. 48.

- [16] DEREICH, S., AND MÜLLER-GRONBACH, T. General multilevel adaptations for stochastic approximation algorithms of Robbins-Monro and Polyak-Ruppert type. *Numer. Math.* *142*, 2 (2019), 279–328.
- [17] E, W., HAN, J., AND JENTZEN, A. Deep learning-based numerical methods for high-dimensional parabolic partial differential equations and backward stochastic differential equations. *Commun. Math. Stat.* *5*, 4 (2017), 349–380.
- [18] E, W., HAN, J., AND JENTZEN, A. Algorithms for solving high dimensional PDEs: from nonlinear Monte Carlo to machine learning. *Nonlinearity* *35*, 1 (2021), 278.
- [19] GADAT, S., AND PANLOUP, F. Optimal non-asymptotic bound of the Ruppert-Polyak averaging without strong convexity. [arXiv:1709.03342](https://arxiv.org/abs/1709.03342) (2017), 41 pages.
- [20] GERMAIN, M., PHAM, H., AND WARIN, X. Neural networks-based algorithms for stochastic control and PDEs in finance. [arXiv:2101.08068](https://arxiv.org/abs/2101.08068) (2021), 27 pages.
- [21] GUO, H., JIN, J., AND LIU, B. Stochastic weight averaging revisited. *Applied Sciences* *13*, 5 (2023), 2935.
- [22] HAN, J., JENTZEN, A., AND E, W. Solving high-dimensional partial differential equations using deep learning. *Proc. Natl. Acad. Sci. USA* *115*, 34 (2018), 8505–8510.
- [23] HE, K., ZHANG, X., REN, S., AND SUN, J. Deep residual learning for image recognition. In *Proceedings of the IEEE Conference on Computer Vision and Pattern Recognition (CVPR)* (2016).
- [24] HU, R., AND LAURIÈRE, M. Recent developments in machine learning methods for stochastic control and games. *Numer. Algebra Control Optim.* *14*, 3 (2024), 435–525.
- [25] IZMAILOV, P., PODOPRIKHIN, D., GARIPPOV, T., VETROV, D., AND WILSON, A. G. Averaging weights leads to wider optima and better generalization. [arXiv:1803.05407](https://arxiv.org/abs/1803.05407) (2018), 12 pages.
- [26] JENTZEN, A., KUCKUCK, B., AND VON WURSTEMBERGER, P. Mathematical Introduction to Deep Learning: Methods, Implementations, and Theory. [arXiv:2310.20360](https://arxiv.org/abs/2310.20360) (2023), 601 pages.
- [27] KINGMA, D. P., AND BA, J. Adam: A method for stochastic optimization. [arXiv:1412.6980](https://arxiv.org/abs/1412.6980) (2014), 15 pages.
- [28] LI, H., RAKHLIN, A., AND JADBABAIE, A. Convergence of Adam Under Relaxed Assumptions. [arXiv:2304.13972](https://arxiv.org/abs/2304.13972) (2023), 35 pages.

- [29] LIU, Y., HAN, T., MA, S., ZHANG, J., YANG, Y., TIAN, J., HE, H., LI, A., HE, M., LIU, Z., WU, Z., ZHAO, L., ZHU, D., LI, X., QIANG, N., SHEN, D., LIU, T., AND GE, B. Summary of ChatGPT-related research and perspective towards the future of large language models. *arXiv:2304.01852* (2023), 21 pages.
- [30] MANDT, S., HOFFMAN, M. D., AND BLEI, D. M. Stochastic gradient descent as approximate Bayesian inference. *arXiv:1704.04289* (2017), 35 pages.
- [31] MORALES-BROTONS, D., VOGELS, T., AND HENDRIKX, H. Exponential moving average of weights in deep learning: Dynamics and benefits. *Transactions on Machine Learning Research* (2024).
- [32] PASZKE, A., GROSS, S., CHINTALA, S., CHANAN, G., YANG, E., DEVITO, Z., LIN, Z., DESMAISON, A., ANTIGA, L., AND LERER, A. Automatic differentiation in PyTorch. <https://openreview.net/forum?id=BJJsrnfCZ> (2017), 4 pages.
- [33] PASZKE, A., GROSS, S., MASSA, F., LERER, A., BRADBURY, J., CHANAN, G., KILLEEN, T., LIN, Z., GIMELSHEIN, N., ANTIGA, L., DESMAISON, A., KÖPF, A., YANG, E., DEVITO, Z., RAISON, M., TEJANI, A., CHILAMKURTHY, S., STEINER, B., FANG, L., BAI, J., AND CHINTALA, S. PyTorch: An imperative style, high-performance deep learning library. *arXiv:1912.01703* (2019), 12 pages.
- [34] POLYAK, B. T. A new method of stochastic approximation type. *Avtomat. i Telemekh.*, 7 (1990), 98–107.
- [35] POLYAK, B. T., AND JUDITSKY, A. B. Acceleration of stochastic approximation by averaging. *SIAM J. Control Optim.* 30, 4 (1992), 838–855.
- [36] PYTORCH-CONTRIBUTORS, C. Adam - PyTorch 2.5 documentation. <https://pytorch.org/docs/stable/generated/torch.optim.Adam.html> (2023), Access date January 5, 2025.
- [37] RAMESH, A., PAVLOV, M., GOH, G., GRAY, S., VOSS, C., RADFORD, A., CHEN, M., AND SUTSKEVER, I. Zero-shot text-to-image generation. *arXiv:2102.12092* (2021), 20 pages.
- [38] REDDI, S. J., KALE, S., AND KUMAR, S. On the Convergence of Adam and Beyond. *arXiv:1904.09237* (2019), 23 pages.
- [39] ROMBACH, R., BLATTMANN, A., LORENZ, D., ESSER, P., AND OMMER, B. High-resolution image synthesis with latent diffusion models. *arXiv:2112.10752* (2022), 45 pages.
- [40] RUDER, S. An overview of gradient descent optimization algorithms. *arXiv:1609.04747* (2017), 14 pages.

- [41] RUPPERT, D. Efficient estimations from a slowly convergent Robbins-Monro process. *Cornell University Operations Research and Industrial Engineering*, hdl.handle.net/1813/8664 (1988), 1–34.
- [42] SAHARIA, C., CHAN, W., SAXENA, S., LI, L., WHANG, J., DENTON, E., GHASEMIPOUR, S. K. S., AYAN, B. K., MAHDAVI, S. S., LOPES, R. G., SALIMANS, T., HO, J., FLEET, D. J., AND NOROUZI, M. Photorealistic Text-to-Image Diffusion Models with Deep Language Understanding. [arXiv:2205.11487](https://arxiv.org/abs/2205.11487) (2022), 46 pages.
- [43] SANDLER, M., ZHMOGINOV, A., VLADYMYROV, M., AND MILLER, N. Training trajectories, mini-batch losses and the curious role of the learning rate. [arXiv:2301.02312](https://arxiv.org/abs/2301.02312) (2023), 21 pages.
- [44] SUN, R. Optimization for deep learning: theory and algorithms. [arXiv:1912.08957](https://arxiv.org/abs/1912.08957) (2017), 60 pages.
- [45] ZHANG, S., CHOROMANSKA, A., AND LECUN, Y. Deep learning with Elastic Averaging SGD. [arXiv:1412.6651](https://arxiv.org/abs/1412.6651) (2014), 24 pages.